# LETTERS

# Presenilins are essential for regulating neurotransmitter release

Chen Zhang[1,2], Bei Wu[1], Vassilios Beglopoulos[1], Mary Wines-Samuelson[1], Dawei Zhang[1], Ioannis Dragatsis[3], Thomas C. Südhof[2] & Jie Shen[1]

Mutations in the presenilin genes are the main cause of familial Alzheimer's disease. Loss of presenilin activity and/or accumulation of amyloid-β peptides have been proposed to mediate the pathogenesis of Alzheimer's disease by impairing synaptic function[1–5]. However, the precise site and nature of the synaptic dysfunction remain unknown. Here we use a genetic approach to inactivate presenilins conditionally in either presynaptic (CA3) or postsynaptic (CA1) neurons of the hippocampal Schaeffer-collateral pathway. We show that long-term potentiation induced by theta-burst stimulation is decreased after presynaptic but not postsynaptic deletion of presenilins. Moreover, we found that presynaptic but not postsynaptic inactivation of presenilins alters short-term plasticity and synaptic facilitation. The probability of evoked glutamate release, measured with the open-channel NMDA (N-methyl-D-aspartate) receptor antagonist MK-801, is reduced by presynaptic inactivation of presenilins. Notably, depletion of endoplasmic reticulum $Ca^{2+}$ stores by thapsigargin, or blockade of $Ca^{2+}$ release from these stores by ryanodine receptor inhibitors, mimics and occludes the effects of presynaptic presenilin inactivation. Collectively, these results indicate a selective role for presenilins in the activity-dependent regulation of neurotransmitter release and long-term potentiation induction by modulation of intracellular $Ca^{2+}$ release in presynaptic terminals, and further suggest that presynaptic dysfunction might be an early pathogenic event leading to dementia and neurodegeneration in Alzheimer's disease.

Conditional inactivation of presenilins in excitatory neurons of the mouse postnatal forebrain causes synaptic dysfunction, memory impairment and age-dependent neurodegeneration[3,6]. Before the onset of neurodegeneration, paired-pulse facilitation, long-term potentiation (LTP) and NMDA receptor (NMDAR)-mediated responses are altered[3], suggesting that synaptic defects caused by the loss of presenilins may be a cellular precursor of neuronal cell death. To determine the precise synaptic site of presenilin function, we performed a systematic genetic analysis by the restriction of presenilin inactivation to hippocampal CA1 or CA3 neurons. This strategy allowed selective examination of the effects of presenilin inactivation in either presynaptic or postsynaptic neurons of the Schaeffer-collateral pathway.

We crossed homozygous floxed presenilin 1 (Psen1), presenilin 2 (Psen2)-null mice (known as fPsen1/fPsen1;Psen2^{−/−}) to Camk2a-Cre[7] and Grik4-Cre (also known as KA1-Cre)[8] transgenic mice to produce CA1- and CA3-restricted presenilin conditional double knockout (Psen cDKO) mice. In situ hybridization confirmed the selective loss of Psen1 expression in CA1 and CA3 neurons of CA1- and CA3-Psen cDKO mice, respectively, at 2 months of age (Fig. 1a). We also crossed Camk2a-Cre and Grik4-Cre mice to Rosa26-lacZ reporter transgenic mice, and observed the expected patterns of CA1- and CA3-restricted β-galactosidase expression (Fig. 1b).

We next examined the effect of selective presenilin inactivation in CA1 or CA3 neurons on theta-burst stimulation (TBS)-induced LTP, which is impaired in Psen cDKO mice lacking presenilin in both CA3 and CA1 neurons[3]. Surprisingly, TBS-induced LTP is normal in CA1-Psen cDKO mice but is markedly impaired in CA3-Psen cDKO mice (Fig. 1c). Thus, presynaptic but not postsynaptic presenilins are required for TBS-induced LTP. To determine whether postsynaptic NMDAR-mediated responses are affected in these mutant mice, we measured AMPA (α-amino-3-hydroxy-5-methyl-4-isoxazole pro-pionic acid) receptor (AMPAR)- and NMDAR-dependent synaptic responses, but detected no change in the NMDAR/AMPAR ratio in CA3- or CA1-Psen cDKO mice (Fig. 1d). Moreover, input–output curves of NMDAR-dependent responses are normal in CA3- and CA1-Psen cDKO mice (Fig. 1e). Thus, loss of presenilin in either presynaptic or postsynaptic neurons alone is insufficient to impair NMDAR-mediated responses. Similarly, input–output coupling (Supplementary Fig. 1) and the current–voltage (I–V) relationship (Supplementary Fig. 2) of AMPAR-mediated synaptic responses are normal in CA3-Psen cDKO mice. These results demonstrate that LTP deficits caused by presynaptic presenilin inactivation are not due to impaired postsynaptic receptor-mediated responses.

We thus investigated whether presynaptic activity is impaired during LTP induction, which could account for the observed LTP deficit. Indeed, we found that short-term depression during the initial stimulus train of TBS is increased in CA3-Psen cDKO mice (Fig. 2a). Paired-pulse facilitation and synaptic frequency facilitation are reduced in CA3-Psen cDKO mice but are normal in CA1-Psen cDKO mice (Fig. 2b, c), which are confirmed by whole-cell recordings (Supplementary Figs 3 and 4). Moreover, the deficit in synaptic facilitation in CA3-Psen cDKO mice is calcium-dependent and is rescued by higher external $Ca^{2+}$ concentrations (Fig. 2d and Supplementary Fig. 5). Consistent with previous reports[3,9], inactivation of Psen1 or Psen2 alone is insufficient to alter frequency facilitation or paired-pulse facilitation (Supplementary Figs 6 and 7). The replenishment of the readily releasable pool after depletion is also normal in CA3-Psen cDKO mice (Supplementary Fig. 8), arguing against an impairment of synaptic vesicle recycling as a cause of the decreased synaptic facilitation.

To test directly whether presynaptic inactivation of presenilins alters the probability of glutamate release, we measured the overall release probability using the open channel blocker MK-801, which irreversibly blocks NMDARs after each synaptic release event[10,11]. Thus, during low-frequency stimulation in the presence of MK-801 and AMPAR blockade, the rate at which NMDAR-mediated synaptic responses decline reflects the average release probability of the

[1]Center for Neurologic Diseases, Brigham & Women's Hospital, Program in Neuroscience, Harvard Medical School, Boston, Massachusetts 02115, USA. [2]Department of Molecular and Cellular Physiology, Howard Hughes Medical Institute, Stanford University School of Medicine, Palo Alto, California 94304, USA. [3]Department of Physiology, The University of Tennessee, Health Science Center, Memphis, Tennessee 38163, USA.
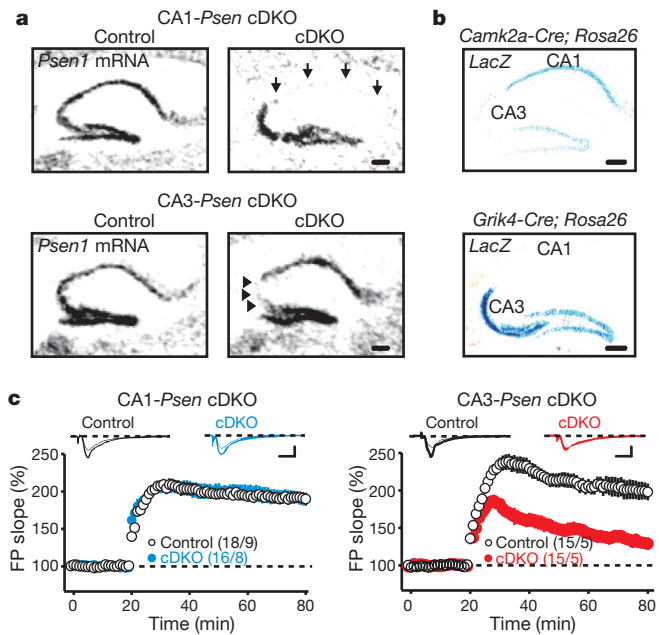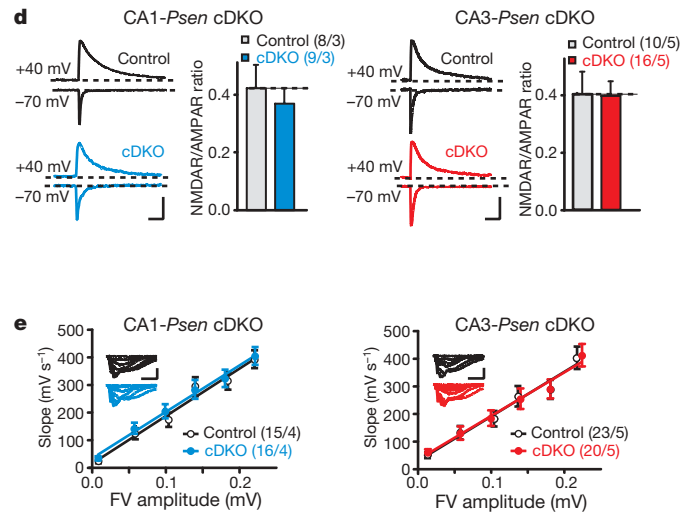
**Figure 1 | Impaired LTP in CA3-*Psen* but not CA1-*Psen* cDKO mice. a**, *In situ* hybridization shows loss of *Psen1* messenger RNA in CA1 (arrows) and CA3 (arrowheads) neurons in CA1-*Psen* and CA3-*Psen* cDKO mice, respectively. Scale bars, 200 μm. **b**, X-gal staining shows absence of Cre-mediated recombination in CA3 and CA1 neurons of *Camk2a-Cre; Rosa26-lacZ* and *Grik4-Cre; Rosa26-lacZ* mice, respectively. Scale bars, 200 μm. **c**, TBS-induced LTP in CA1-*Psen* cDKO (filled blue circles) and CA3-*Psen* cDKO (filled red circles) compared to their controls (open circles). Representative traces before (thin) and after (thick) LTP induction are shown. Superimposed traces are averages of four consecutive responses 1 min before and 60 min after TBS. FP, field potential. Scale bars, 10 ms, 1 mV. **d**, Normal ratio of NMDAR to AMPAR responses in CA3-*Psen* and CA1-*Psen* cDKO mice. Scale bars, 200 ms, 200 pA. **e**, NMDAR-mediated input–output curves. FV, fibre volley. Scale bars, 40 ms, 1 mV. All data represent mean and s.e.m. The values in parentheses indicate the number of hippocampal neurons or slices (left) and the number of mice (right) used in each experiment.
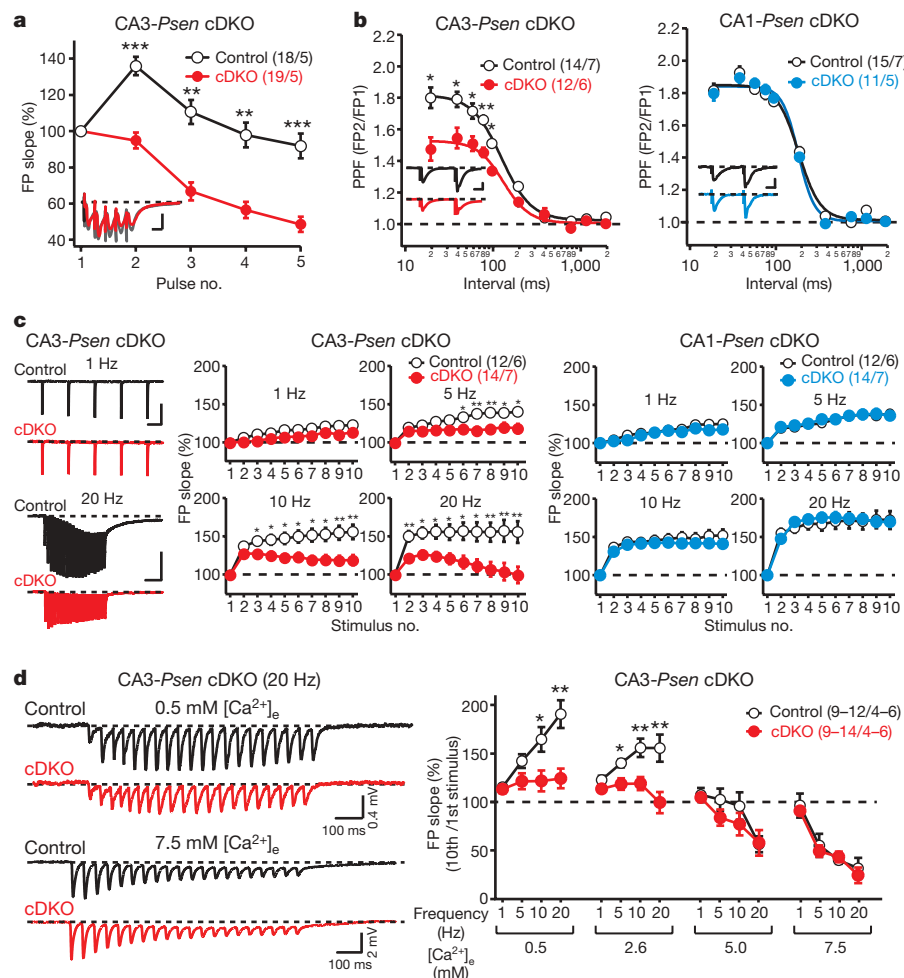


**Figure 2 | Presynaptic defects in CA3-*Psen* but not CA1-*Psen* cDKO mice. a**, Reduced facilitation of field excitatory postsynaptic potential (fEPSP) slope during single TBS in CA3-*Psen* cDKO mice. Inset shows representative traces of field responses during single TBS stimulus train. FP, field potential. Scale bar, 10 ms, 2 mV. **b**, Paired-pulse facilitation (PPF) in CA3- and CA1-*Psen* cDKO mice. Scale bars in insets, 10 ms, 0.5 mV. **c**, Synaptic facilitation elicited by stimulus trains of indicated frequencies in CA3- and CA1-*Psen* cDKO mice. Scale bars, 2 mV, 500 ms (top); 2 mV, 250 ms (bottom). **d**, Calcium-dependence of frequency facilitation defects in CA3-*Psen* cDKO mice. Scale bars, 0.4 mV, 100 ms (top); 2 mV, 100 ms (bottom). $[Ca^{2+}]_e$ denotes extracellular $Ca^{2+}$ concentration. All data represent mean ± s.e.m. *$P < 0.05$, **$P < 0.01$, ***$P < 0.001$. The values in parentheses indicate the number of hippocampal slices (left) and the number of mice (right) used in each experiment.

synapses. We found that the decay rate of postsynaptic responses as a function of stimulus number is decreased in CA3-*Psen* cDKO mice (Fig. 3a). When these results were fitted to a single exponential as a rough measure of the average release probability, we observed an
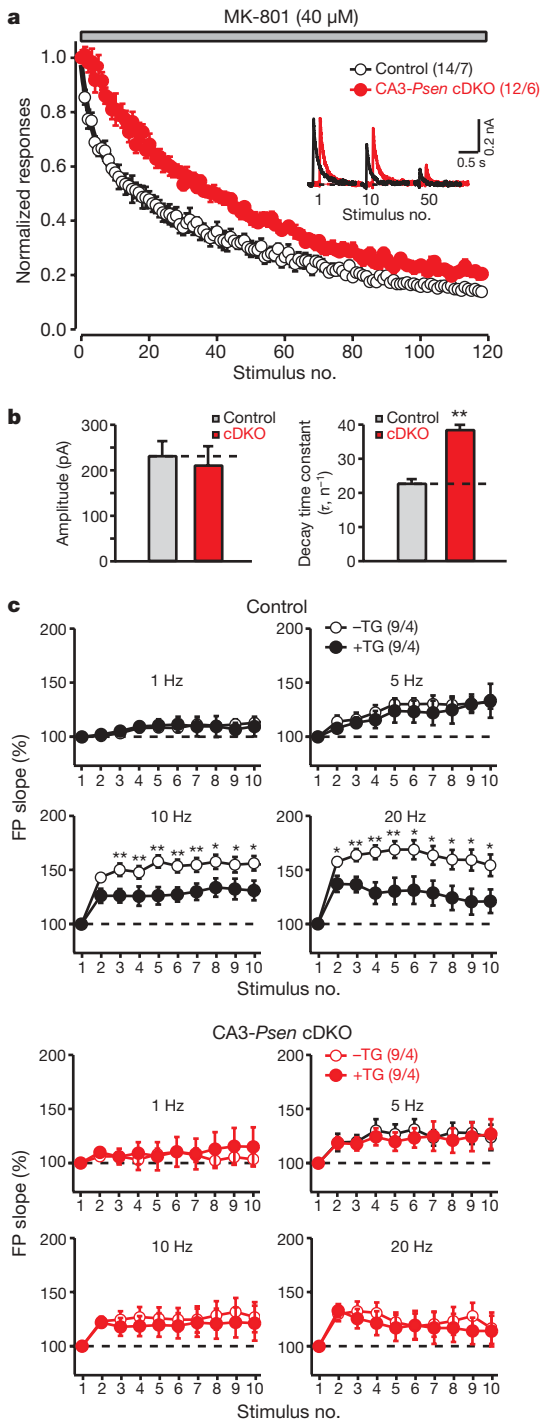


**Figure 3 | Presynaptic presenilin regulates glutamate release by intracellular Ca²⁺ stores. a**, Reduced decay rate of NMDAR-mediated responses in the presence of MK-801 in CA3-*Psen* cDKO mice. Representative traces of EPSCs after the first, tenth and fiftieth stimulus are shown in the inset. **b**, Amplitude of the first NMDAR-mediated response (left) and the decay time constant (right; fitted to a single exponential curve) of the NMDAR-mediated EPSC amplitude in the presence of MK-801. **c**, Effects of thapsigargin (TG) treatment on synaptic facilitation in control and CA3-*Psen* cDKO slices. All data represent mean and s.e.m. $*P < 0.05$, $**P < 0.01$. The values in parentheses indicate the number of hippocampal slices or neurons (left) and the number of mice (right) used in each experiment.

almost twofold increase in the decay constant in CA3-*Psen* cDKO mice (Fig. 3b). This result shows a major decrease in release probability in CA3-*Psen* cDKO mice, demonstrating a critical role for presenilins in regulating the probability of glutamate release. Spontaneous miniature excitatory postsynaptic currents (EPSCs), however, show a normal frequency and amplitude in CA3-*Psen* cDKO mice (Supplementary Fig. 9), suggesting that a defect in Ca²⁺-dependent release may account for the observed presynaptic phenotypes.

Evoked neurotransmitter release is dependent on the local increase in intracellular calcium concentrations. Presynaptic Ca²⁺ increases are caused by Ca²⁺ influx by voltage-gated calcium channels (VGCCs) and by calcium release from intracellular stores[12]. Because changes in Ca²⁺ influx by VGCCs have been reported to affect release probability[10,11], we measured VGCC currents in the somata of CA3 neurons and found an unaltered $I$–$V$ relationship in CA3-*Psen* cDKO mice (Supplementary Fig. 10). Thus, the change in release probability in CA3-*Psen* cDKO mice is unlikely to be due to VGCC dysfunction. Because presenilins have been reported to be involved in the regulation of Ca²⁺ homeostasis in intracellular stores[13–16], we examined the effect of depletion of intracellular Ca²⁺ stores on synaptic facilitation in CA3-*Psen* cDKO mice. Thapsigargin, which irreversibly blocks Ca²⁺ pumps on the endoplasmic reticulum (ER), thereby abolishing intracellular Ca²⁺ release[17], suppresses synaptic facilitation during high-frequency stimulation in control synapses, but has no discernable effect in presenilin-deficient nerve terminals (Fig. 3c). Thus, thapsigargin treatment mimics and occludes the effect of presenilin inactivation on synaptic facilitation, suggesting that dysregulation of intracellular Ca²⁺ release underlies the presynaptic defects in CA3-*Psen* cDKO mice.

Calcium release from the ER is mediated by two main types of receptors: ryanodine receptors (RyRs), which mediate calcium-induced calcium release (CICR), and inositol-1,4,5-triphosphate receptors (InsP₃Rs). We therefore tested the effects of specific inhibitors for RyRs or InsP₃Rs on synaptic facilitation[18–20]. Blockade of RyRs by ryanodine (100 μM) or dantrolene mimics the effect of thapsigargin (Fig. 4a and Supplementary Fig. 11), whereas blockade of InsP₃Rs by xestospongin C has no effect (Supplementary Fig. 12). Thus, a specific defect in RyR-mediated CICR probably underlies the presynaptic impairment in CA3-*Psen* cDKO mice.

To determine directly whether Ca²⁺ homeostasis is indeed affected by presenilin inactivation, we performed Ca²⁺ imaging in cultured hippocampal neurons, in which presenilin is acutely inactivated with a lentivirus expressing Cre recombinase. This postnatal culture system circumvents the requirement of presenilins in neurogenesis during embryonic development[21,22] and permits the direct measurement of Ca²⁺ concentrations in these neurons. Presenilin expression is abolished in Cre-infected (*Psen* cDKO) neurons, but their neuronal and synaptic morphology appear normal (Supplementary Fig. 13a, c). Similar to CA3-*Psen* cDKO mice, presynaptic short-term plasticity measured as paired-pulse ratio is altered in *Psen* cDKO hippocampal neurons (Supplementary Fig. 13b), confirming that this preparation recapitulates the presynaptic defect of the presenilin-deficient hippocampus. We then measured cytosolic calcium concentration ($[Ca^{2+}]_i$) changes elicited by depolarization (80 mM KCl), which are contributed by both Ca²⁺ influx through VGCCs and Ca²⁺ efflux from intracellular stores. The amplitude of $[Ca^{2+}]_i$ changes ($\Delta[Ca^{2+}]_i$) elicited by depolarization is reduced in *Psen* cDKO neurons (Fig. 4b and Supplementary Fig. 14). Blockade of RyRs with ryanodine (100 μM) in control neurons mimics the effect of presenilin inactivation, whereas ryanodine has no further effect in *Psen* cDKO neurons (Fig. 4b and Supplementary Fig. 14). Thus, blockade of RyRs mimics and occludes the effect of presenilin inactivation on depolarization-induced $[Ca^{2+}]_i$ changes. Blockade of InsP₃R with xestospongin C, however, has no effect (Fig. 4b and Supplementary Fig. 14). These results directly show that presenilin inactivation in
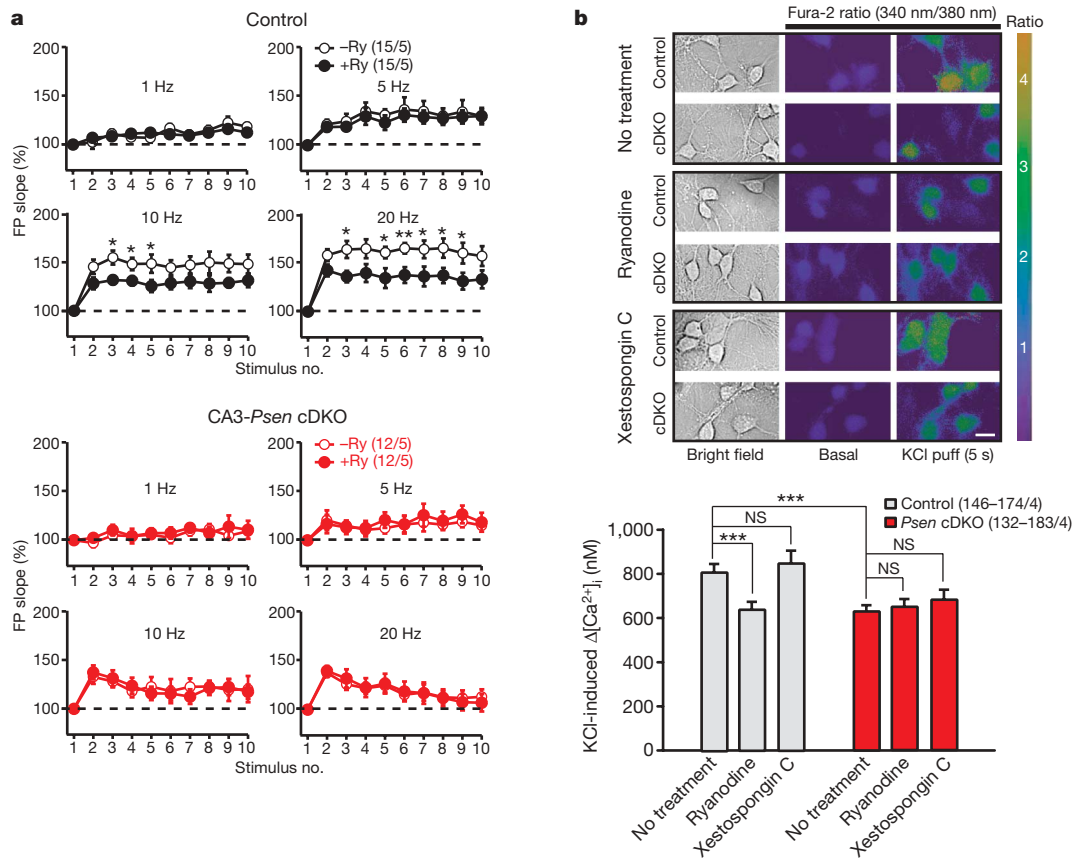
**Figure 4 | Blockade of RyRs mimics and occludes the defects in synaptic facilitation and calcium homeostasis in CA3-*Psen* cDKO hippocampal slices and cultured *Psen* cDKO hippocampal neurons. a**, Effect of ryanodine (Ry; 100 μM) treatment on synaptic facilitation in control and CA3-*Psen* cDKO mice. **b**, Effect of ryanodine (100 μM) or xestospongin C (1 μM) treatment on depolarization-induced $[Ca^{2+}]_i$ increases in cultured hippocampal neurons. Representative calcium images (top) show high potassium (80 mM)-induced $Ca^{2+}$ responses in control and *Psen* cDKO neurons. Scale bar, 20 μm. All data represent mean and s.e.m. *$P < 0.05$, **$P < 0.01$, ***$P < 0.001$. The values in parentheses indicate the number of hippocampal slices or neurons (left) and the number of mice (right) used in each experiment.

neurons impairs depolarization-induced $Ca^{2+}$ increases that involve RyR-dependent CICR.

Collectively, our studies demonstrate that the loss of presenilin impairs LTP induction and glutamatergic neurotransmitter release in mature neurons by a presynaptic mechanism (see model in Supplementary Fig. 15). Our pharmacological and imaging studies, coupled with electrophysiological analysis, further show that a specific impairment in RyR-mediated CICR underlies the presynaptic defects caused by the loss of presenilin. Therefore, the presynaptic function of presenilin unexpectedly acts, at least in part, on the RyR-mediated $Ca^{2+}$ release from intracellular stores. Furthermore, our data suggest that short- and long-term plasticity in the hippocampus depend partly on intracellular $Ca^{2+}$ release, which regulates neurotransmitter release.

Previous studies investigating synaptic dysfunction in the pathophysiology of Alzheimer's disease have uncovered defects in NMDARs and AMPARs, leading to the notion that postsynaptic impairment may be the early pathogenic change in this disease[3,23,24]. However, the possibility that impaired presynaptic function may be the primary synaptic defect in Alzheimer's disease was largely unexplored. The β-amyloid precursor protein (APP) and amyloid-β peptides were reported to be presynaptically localized and were implicated in vesicle recycling[25–27]. Our findings, which distinguish unequivocally between presynaptic and postsynaptic functions of presenilin, raise the possibility that presynaptic mechanisms are involved in Alzheimer's disease pathophysiology. This hypothesis is supported by the findings that presenilin is localized to presynaptic terminals (Supplementary Fig. 16), and that APP carboxy-terminal fragments, which are substrates of presenilin-dependent γ-secretase activity and precursors of amyloid-β, accumulate in presynaptic

terminals of *Psen1* cKO mice[28]. Intriguingly, gene products responsible for recessively inherited familial Parkinson's disease, such as DJ-1 (also known as PARK7) and PINK1, are required for evoked dopamine release from nigrostriatal terminals[29,30]. These findings suggest that defects in presynaptic neurotransmitter release may represent a general convergent mechanism leading to neurodegeneration.

## METHODS SUMMARY

**Electrophysiological analysis.** Acute hippocampal slices (400 μm) were prepared as described previously[3]. Synaptic strength was quantified as the initial slope of field potentials recorded with artificial cerebrospinal fluid (aCSF)-filled microelectrodes (1–2 MΩ). Intracellular whole-cell recordings were performed using Multiclamp 700B in CA1 or CA3 pyramidal neurons. Data were analysed using Igor and Clampfit. Experimenters were blinded to the genotypes of the mice.

**Hippocampal neuronal culture.** *Psen* cDKO hippocampal neuronal cultures were derived from *fPsen1/fPsen1;Psen2*$^{-/-}$ pups at postnatal day 1, followed by infection of lentiviral vectors expressing either a functional Cre–GFP or a mutant Cre–GFP fusion protein at 2 days *in vitro* (DIV) for 72 h. Whole-cell patch recordings from cultured hippocampal neurons at 13–15 DIV were performed at room temperature using a Multiclamp 700B amplifier with pCLAMP acquisition software.

**$Ca^{2+}$ imaging.** Hippocampal neurons were loaded with Fura-2 AM, and imaged with a Leica DMI6000 Microscope with a ×40 lens. Imaging processing and data analysis were performed using LAS AF software. High concentrations of potassium were applied using an eight-channel gravity perfusion system.

**Full Methods** and any associated references are available in the online version of the paper at www.nature.com/nature.

1. Hardy, J. & Selkoe, D. J. The amyloid hypothesis of Alzheimer's disease: progress and problems on the road to therapeutics. *Science* 297, 353–356 (2002).

2.  Hsia, A. Y. et al. Plaque-independent disruption of neural circuits in Alzheimer's disease mouse models. Proc. Natl Acad. Sci. USA 96, 3228–3233 (1999).
3.  Saura, C. A. et al. Loss of presenilin function causes impairments of memory and synaptic plasticity followed by age-dependent neurodegeneration. Neuron 42, 23–36 (2004).
4.  Selkoe, D. J. Alzheimer's disease is a synaptic failure. Science 298, 789–791 (2002).
5.  Shen, J. & Kelleher, R. J. III. The presenilin hypothesis of Alzheimer's disease: evidence for a loss-of-function pathogenic mechanism. Proc. Natl Acad. Sci. USA 104, 403–409 (2007).
6.  Feng, R. et al. Forebrain degeneration and ventricle enlargement caused by double knockout of Alzheimer's presenilin-1 and presenilin-2. Proc. Natl Acad. Sci. USA 101, 8162–8167 (2004).
7.  Zakharenko, S. S. et al. Presynaptic BDNF required for a presynaptic but not postsynaptic component of LTP at hippocampal CA1–CA3 synapses. Neuron 39, 975–990 (2003).
8.  Nakazawa, K. et al. Requirement for hippocampal CA3 NMDA receptors in associative memory recall. Science 297, 211–218 (2002).
9.  Yu, H. et al. APP processing and synaptic plasticity in presenilin-1 conditional knockout mice. Neuron 31, 713–726 (2001).
10. Hessler, N. A., Shirke, A. M. & Malinow, R. The probability of transmitter release at a mammalian central synapse. Nature 366, 569–572 (1993).
11. Rosenmund, C., Clements, J. D. & Westbrook, G. L. Nonuniform probability of glutamate release at a hippocampal synapse. Science 262, 754–757 (1993).
12. Emptage, N. J., Reid, C. A. & Fine, A. Calcium stores in hippocampal synaptic boutons mediate short-term plasticity, store-operated $Ca^{2+}$ entry, and spontaneous transmitter release. Neuron 29, 197–208 (2001).
13. Chan, S. L., Mayne, M., Holden, C. P., Geiger, J. D. & Mattson, M. P. Presenilin-1 mutations increase levels of ryanodine receptors and calcium release in PC12 cells and cortical neurons. J. Biol. Chem. 275, 18195–18200 (2000).
14. Green, K. N. et al. SERCA pump activity is physiologically regulated by presenilin and regulates amyloid beta production. J. Cell Biol. 181, 1107–1116 (2008).
15. Stutzmann, G. E., Caccamo, A., LaFerla, F. M. & Parker, I. Dysregulated IP3 signaling in cortical neurons of knock-in mice expressing an Alzheimer's-linked mutation in presenilin1 results in exaggerated $Ca^{2+}$ signals and altered membrane excitability. J. Neurosci. 24, 508–513 (2004).
16. Tu, H. et al. Presenilins form ER $Ca^{2+}$ leak channels, a function disrupted by familial Alzheimer's disease-linked mutations. Cell 126, 981–993 (2006).
17. Treiman, M., Caspersen, C. & Christensen, S. B. A tool coming of age: thapsigargin as an inhibitor of sarco-endoplasmic reticulum $Ca^{2+}$-ATPases. Trends Pharmacol. Sci. 19, 131–135 (1998).
18. Gafni, J. et al. Xestospongins: potent membrane permeable blockers of the inositol 1,4,5-trisphosphate receptor. Neuron 19, 723–733 (1997).
19. Meissner, G. Ryanodine activation and inhibition of the $Ca^{2+}$ release channel of sarcoplasmic reticulum. J. Biol. Chem. 261, 6300–6306 (1986).
20. Stutzmann, G. E. et al. Enhanced ryanodine receptor recruitment contributes to $Ca^{2+}$ disruptions in young, adult, and aged Alzheimer's disease mice. J. Neurosci. 26, 5180–5189 (2006).
21. Handler, M., Yang, X. & Shen, J. Presenilin-1 regulates neuronal differentiation during neurogenesis. Development 127, 2593–2606 (2000).
22. Shen, J. et al. Skeletal and CNS defects in Presenilin-1-deficient mice. Cell 89, 629–639 (1997).
23. Kamenetz, F. et al. APP processing and synaptic function. Neuron 37, 925–937 (2003).
24. Snyder, E. M. et al. Regulation of NMDA receptor trafficking by amyloid-β. Nature Neurosci. 8, 1051–1058 (2005).
25. Buxbaum, J. D. et al. Alzheimer amyloid protein precursor in the rat hippocampus: transport and processing through the perforant path. J. Neurosci. 18, 9629–9637 (1998).
26. Lazarov, O., Lee, M., Peterson, D. A. & Sisodia, S. S. Evidence that synaptically released β-amyloid accumulates as extracellular deposits in the hippocampus of transgenic mice. J. Neurosci. 22, 9785–9793 (2002).
27. Yao, P. J. & Coleman, P. D. Reduced O-glycosylated clathrin assembly protein AP180: implication for synaptic vesicle recycling dysfunction in Alzheimer's disease. Neurosci. Lett. 252, 33–36 (1998).
28. Saura, C. A. et al. Conditional inactivation of presenilin 1 prevents amyloid accumulation and temporarily rescues contextual and spatial working memory impairments in amyloid precursor protein transgenic mice. J. Neurosci. 25, 6755–6764 (2005).
29. Goldberg, M. S. et al. Nigrostriatal dopaminergic deficits and hypokinesia caused by inactivation of the familial Parkinsonism-linked gene DJ-1. Neuron 45, 489–496 (2005).
30. Kitada, T. et al. Impaired dopamine release and synaptic plasticity in the striatum of PINK1-deficient mice. Proc. Natl Acad. Sci. USA 104, 11441–11446 (2007).

## METHODS

**Generation of CA1-*Psen* and CA3-*Psen* cDKO mice.** CA1-*Psen* and CA3-*Psen* cDKO mice contain homozygous floxed *Psen1* alleles, homozygous *Psen2$^{-/-}$* alleles, and the *Camk2a-Cre*[7] and *Grik4-Cre*[8] transgene, respectively. Because *Psen2$^{-/-}$* mice have no detectable phenotypes[31], it was unnecessary to generate floxed *Psen2* mice. For each cDKO mouse line, *fPsen1/fPsen1;Psen2$^{-/-}$;Cre* mice were bred with *fPsen1/fPsen1;Psen2$^{-/-}$* mice to obtain more cDKO mice (*fPsen1/fPsen1;Psen2$^{-/-}$;Cre*) and *fPsen1/fPsen1;Cre* were bred with *fPsen1/fPsen1* to obtain control mice (*fPsen1/fPsen1*). The introduction of two *loxP* sites into *Psen1* introns 1 and 3 was previously confirmed not to affect transcription, splicing or translation[9]. The genetic background of these mice was similar in the C57BL6/129 hybrid background, with breeding carried out similarly for both groups. All procedures relating to animal care and treatment conformed to the Institutional and NIH guidelines.

***In situ* hybridization and LacZ staining.** *In situ* hybridization was carried out as previous described using a 260-base-pair (bp) sense or antisense riboprobe specific for *Psen1* exons 2 and 3 (ref. 32). For X-gal staining, *Camk2a-Cre* and *Grik4-Cre* transgenic mice were bred to *Rosa26-lacZ* mice, and double transgenic offspring containing both the *Cre* and the *lacZ* transgenes were analysed.

**Field and whole-cell electrophysiological analysis of acute hippocampal slices.** All electrophysiological analysis was performed by experimenters who were blinded to the genotypes of the mice. Acute hippocampal slices (400 μm) were prepared as described before[3]. The slices were maintained in a storage chamber containing aCSF (124 mM NaCl, 5 mM KCl, 1.25 mM NaH$_2$PO$_4$, 1.3 mM MgCl$_2$, 2.6 mM CaCl$_2$, 26 mM NaHCO$_3$, 10 mM dextrose, pH 7.4, 300–310 mOsM) at 30 °C. Stimulation (500 μs) pulses were delivered with a bipolar concentric metal electrode. Synaptic strength was quantified as the initial slope of field potentials recorded with aCSF-filled microelectrodes (1–2 MΩ). In LTP recordings, baseline responses were collected every 15 s with a stimulation intensity that yielded 60% of maximal response. LTP was induced by five episodes of TBS delivered at 0.1 Hz. Each episode contains ten stimulus trains (five pulses at 100 Hz) delivered at 5 Hz. Average responses (mean ± s.e.m.) are expressed as percentage of pre-TBS baseline response. Synaptic facilitations were measured as the percentage of the fEPSP slope versus the first fEPSP slope at a given stimulus train in individual slices.

Intracellular (whole-cell) recordings were performed using Multiclamp 700B (Molecular device) in CA1 or CA3 pyramidal neurons. Patch pipettes (3–5 MΩ) were filled with internal solution consisting of (in mM): 110 Cs-methanesulphonate, 20 tetraethylammonium-chloride, 8 KCl, 10 EGTA, 10 HEPES, 5 QX-314 (a derivative of lidocaine), 3 Mg-ATP, 0.3 Na$_2$GTP, pH 7.3; 275–285 mOsM. AMPAR responses were recorded in the presence of 50 μM DL-2-amino-5-phosphonovaleric acid and 100 μM picrotoxin to block NMDAR- and GABA (γ-aminobutyric acid) type A receptor-mediated responses, respectively. NMDAR responses were recorded in the presence of 10 μM 6-cyano-7-nitroquinoxaline-2,3-dione (CNQX) and 100 μM picrotoxin to block AMPAR- and GABA type A receptor-mediated responses, respectively. For the MK-801 experiment, recordings of NMDAR-mediated EPSC were made every 20 s before and during exposure to MK-801 (40 μM). The NMDAR-mediated EPSC amplitude was plotted as a function of stimulus number. Decay curves were normalized to the amplitude of the first EPSC in the presence of MK-801 and were fitted to a single exponential curve to estimate the decay time course. NMDA-mediated EPSC was measured at +40 mV, and was elicited by focal stimulation in the presence of CNQX (10 μM) and picrotoxin (100 μM). To record calcium current through VGCCs, tetrodotoxin (extracellular, 500 nM) and QX-314 (intracellular, 5 mM) were used to block sodium current; Cs$^+$ (intracellular, 110 mM) and tetraethyl-lammonium (intracellular, 20 mM) were used to block potassium current. To measure the synaptic facilitation, values of the fEPSP slope (second to tenth responses in a 20-pulse stimulus train) were normalized to the slope of the first fEPSP of the stimulus train. Data were analysed using Igor (Wavemetrics) and Clampfit (Molecular device).

***Psen* cDKO hippocampal neuronal cultures.** To circumvent the requirement of presenilin in neurogenesis during embryonic development[21,22], we established *Psen* cDKO hippocampal neuronal cultures derived from *fPsen1/fPsen1;*

*Psen2$^{-/-}$* newborn pups, followed by infection of lentiviral vectors expressing either a functional Cre–GFP or a mutant Cre–GFP fusion protein. Hippocampi from *fPsen1/fPsen1;Psen2$^{-/-}$* pups were dissected and treated with 0.25% trypsin at 37 °C for 20 min. Cells were plated at a density of 65,000 cells cm$^{-2}$ on poly-D-lysine-coated 35-mm dishes (Costar). Cultures were infected with lentiviruses (300 μl conditioned medium per well in a 24-well plate) expressing at 2 DIV for 72 h. Infected neurons were cultured until 13–15 DIV for further biochemical, morphological, electrophysiological and imaging analyses. Lentiviruses were produced by transfecting human embryonic kidney HEK293 cells (ATCC) with the respective pFUGW vectors and two helper plasmids (pVSVg and pCMVΔ8.9) using FUGENE 6 (Roche), as previously described[33]. Conditioned medium containing viruses was collected 48 h after transfection, and spun (800g for 5 min) to remove HEK cell debris before adding to the neuronal culture.

**Morphological analysis of postnatal hippocampal cultures.** Cultured neurons at 14 DIV were fixed with methanol (−20 °C). Fixed cultures were then incubated with primary antibodies against synaptophysin (monoclonal; 1:2,000; Sigma) and microtubule-activated protein 2 (MAP2; polyclonal; 1:2,000; Sigma). After rinsing three times with PBS, the neurons were incubated with fluorescent secondary antibodies for 30 min. After washing, cultures were mounted with Vectashield mounting medium (Vector labs). Confocal microscopic analysis was performed on a Zeiss LSM 510 microscope. Identical acquisition settings were applied to all samples of the experiment. Images of neurons were collected with a ×40 oil-immersion objective lens. Images were analysed in a genotype-blind manner using the NIH Image/Image J program.

**Whole-cell electrophysiological analysis of postnatal hippocampal cultures.** Whole-cell patch recordings from cultured hippocampal neurons at 13–15 DIV were performed at room temperature using a Multiclamp 700B amplifier (Molecular device) with pCLAMP acquisition software. Synaptic transmission was elicited with a concentric focal stimulus electrode, and EPSCs were recorded with a patch electrode (3–5 MΩ) in whole-cell recording mode and filtered at 2 kHz. Pipette solution contained (in mM): 136.5 K-gluconate, 0.2 EGTA, 10 HEPES, 9 NaCl, 17.5 KCl, 5 QX-314, 4 Mg-ATP and 0.3 Na-GTP (adjusted to pH 7.4 with KOH). The extracellular solution was HEPES-buffered saline containing (in mM): 145 NaCl, 3 KCl, 10 HEPES, 2 CaCl$_2$, 1 MgCl$_2$, 8 dextrose, pH 7.2.

**Calcium imaging analysis.** Hippocampal neurons were loaded with Fura-2 AM (5 μM, 45 min at 37 °C) (Molecular probes), and imaged with a Leica DMI6000 Microscope with ×40 lens (numerical aperture 0.75). The method and parameters for *in vitro* calibration (Invitrogen calibration kit) were as described previously[34]. Imaging processing and data analysis were performed using LAS AF software (Leica). High concentrations of potassium were applied using an 8-channel gravity perfusion system (ALA Scientific Instrument).

**Subcellular fractionation analysis.** For enrichment of synaptic vesicle (presynaptic) proteins, four adult cortices (3-month-old) were homogenized with a Dounce teflon homogenizer in ice-cold buffer containing 0.32 M sucrose, 4 mM HEPES, pH 7.3, and protease and phosphatase inhibitor cocktails. For the P2 fraction, crude homogenates were centrifuged at 800g twice to remove debris, the supernatant were centrifuged at 9,200g, and the pellet was resuspended in 0.32 M sucrose buffer. For the LP1 fraction, P2 synaptosomes were centrifuged at 10,200g, resuspended in 0.32 M sucrose buffer and hypotonically lysed in nine volumes of water. The lysate was centrifuged at 25,000g, and the pellet was resuspended in buffer containing 1% NP-40 to produce LP1. For the LP2 fraction, the supernatant from the LP1 purification step was centrifuged at 165,000g, and the pellet was resuspended in buffer containing 1% NP-40.

31. Steiner, H. *et al.* A loss of function mutation of presenilin-2 interferes with amyloid β-peptide production and notch signaling. *J. Biol. Chem.* **274**, 28669–28673 (1999).
32. Wines-Samuelson, M., Handler, M. & Shen, J. Role of presenilin-1 in cortical lamination and survival of Cajal-Retzius neurons. *Dev. Biol.* **277**, 332–346 (2005).
33. Watanabe, H. *et al.* Indirect regulation of presenilins in CREB-mediated transcription. *J. Biol. Chem.* **284**, 13705–13713 (2009).
34. Zhang, C. & Zhou, Z. Ca$^{2+}$-independent but voltage-dependent secretion in mammalian dorsal root ganglion neurons. *Nature Neurosci.* **5**, 425–430 (2002).